ISSN 1746-7659, England, UK
Journal of Information and Computing Science
Vol. 16, No. 2, 2021, *pp*.126-133

Impact of electrokinetic variable viscosity on peristaltic transfer of Jeffrey fluid

Laxmi Devindrappa and N. B. Naduvinamani
Gulbarga University, Kalaburagi.
(Received March 14, 2021, accepted May 08, 2021)

Abstract. This article presents a mathematical model to study the impact of electro kinetic variable viscosity on peristaltic transfer of Jeffrey fluid. We have considered the non-Newtonian Jeffrey fluid model with the use of linear momentum. Poisson-Boltzmann equations are simplified by using Debye-H$\ddot{u}$ckel linearization approximation. The closed form analytical solutions are presented by using long wavelength and low Reynolds number assumptions. The expressions for pressure rise and pressure gradient are determined by using perturbation method. The influence of various parameters like Jeffrey fluid parameter, Electro-osmotic parameter, Electroosmotic velocity and Viscosity parameter on the flow characteristics are discussed through graphs. It is revealed that with an increase in the Viscosity parameter there is decrease in the pumping, free pumping, enhances in the augmented pumping region and the axial pressure gradient decreases with increasing Viscosity.

Keywords: Jeffrey fluid, Electro-osmotic, Electroosmotic velocity and Viscosity parameter

1. Introduction

The phenomena of peristaltic are of great importance in many engineering and biological systems. Latham [1] has coined the idea of fluid transport by means of peristaltic waves in mechanical and physiological studies. Peristaltic flow of non-Newtonian fluids in a tube was first studied by Raju and Devanathan [2]. Information on the topic is quite reasonable and researchers mention a few recent representative attempts and several useful references in their investigations [3-8].

Divya et al. [9] described the hemodynamics of variable liquid properties on the MHD peristaltic mechanism of Jeffery fluid with heat and mass transfer. Here it is observed that increase in the variable viscosity parameter is found to accelerate the fluid flow. Abbasi et al. [10] described the hydro magnetic peristaltic transport of copper-water nanofluid with temperature-dependent effective viscosity. Their analysis shows that, pressure gradient in the wider part of the channel is found to increase as a function of the variable viscosity. Akbar and Nadeem [11] have analyzed the simulation of variable viscosity and Jeffrey fluid model for blood flow through a tapered artery with a stenosis. Farooq et al. [12] studied the magneto hydrodynamic peristalsis of variable viscosity Jeffrey fluid with heat and mass transfer. It is noticed that velocity has small resistance in the case of variable viscosity. Nadeem and Akbar [13] discussed the peristaltic flow of a Jeffrey fluid with Variable Viscosity in an asymmetric channel.

Flow of fluids in channels under the effect of an electrical field is a key area in both medical engineering and energy sciences. R. E Abo-Elkhalr et al. [14] studied combine impacts of electro kinetic variable viscosity and partial slip on peristaltic MHD flow through a Micro-Channel, observing that they are especially used to relieve pain and also to accelerate fracture healing in bones. These remedial procedures have also been employed to accelerate the flow of blood. Laxmi et al. [15] studied the peristaltically induced Electroosmotic flow of Jeffrey fluid with Zeta potential and Navier- Slip at the wall. Electrokinetic flow of peristaltic transport of Jeffrey fluid in a porous channel analyzed by Laxmi et al. [16]. Microchannels are used in fluid control. Sharma et al. [17] demonstrated the analysis of double diffusive convection in electroosmosis regulated peristaltic transport of nanofluids. Their analysis can be utilized in clinical significances like drug delivery systems, cell therapeutics and particles filtrations. Some researchers studied on microchannel [18-20].

In this paper the impact of electro kinetic variable viscosity on peristaltic transfer of Jeffrey fluid were investigated. Consider the approximation of long wavelength and low Reynolds number, the governing flow problem is simplified by using perturbation method. The resulting equations are solved analytically and exact solutions are presented. The impact of all the physical parameters of interest is taken into consideration with the help of graphs.

2. Mathematical model

Consider an incompressible Jeffrey fluid in a two dimensional micro-channel of width $2a$. The sinusoidal wave trains propagate along the channel wall with constant speed c and propped the fluid along the walls. In a regular co-ordinate system (X, Y), the geometry of the wall surface is described by

$$H(x,t) = a + b\cos\frac{2\pi}{\lambda}(X - ct). \tag{1}$$

where b is amplitude of the waves and λ is the wave length, c is the velocity of wave propagation and X is the direction of wave propagation.

The constitutive equations for Jeffrey fluid are given by

$$\overline{T} = -P\overline{I} + \overline{S}\ . \tag{2}$$

$$\overline{S} = \frac{\mu(\overline{Y})}{1+\lambda_1}\left(\dot{\gamma} + \lambda_2\ddot{\gamma}\right). \tag{3}$$

where $\overline{T}$ and $\overline{S}$ are the Cauchy stress tensor and extra stress tensor, $\overline{P}$ is the pressure, $\overline{I}$ is the identity tensor, μ is the dynamic viscosity, λ_1 is the ratio of relaxation to retardation times, λ_2 λ_2 is the retardation time, $\dot{\gamma}$ is the shear rate and dots over the quantities denote differentiation.

Under the assumptions that the channel length is an integral multiple of the wave length λ and the pressure difference across the ends of the channel is a constant, the flow is inherently unsteady in the laboratory frame $(\overline{X}, \overline{Y})$and become steady in the wave frame$(\bar{x}, \bar{y})$ which is moving with velocity c along the wave. The transformation between these two frames is given by $x = \overline{X} - ct, y = \overline{Y}, u = \overline{U}, v = \overline{V}$. (4)

Where U and V are velocity components within in the laboratory frame and u and v are the velocity components within the wave frame.

The equations governing the electro osmotic flow are taken as

$$\frac{\partial u}{\partial x} + \frac{\partial v}{\partial y} = 0. \tag{5}$$

$$\rho\left[u\frac{\partial u}{\partial x} + v\frac{\partial u}{\partial y}\right] = -\frac{\partial p}{\partial x} + \frac{\partial \tau_{xx}}{\partial x} + \frac{\partial \tau_{xy}}{\partial y} - \frac{\mu}{k}(u + c) + \rho_e E_x. \tag{6}$$

$$\rho\left[u\frac{\partial v}{\partial x} + v\frac{\partial v}{\partial y}\right] = -\frac{\partial p}{\partial y} + \frac{\partial \tau_{xy}}{\partial x} + \frac{\partial \tau_{yy}}{\partial y}. \tag{7}$$

where E_x denote electro kinetic body force. The Poisson's equation is defined as

$$\Delta^2\Phi = -\frac{\rho_e}{\varepsilon}. \tag{8}$$

in which k is the permeability of the porous medium, ρ_e is the density of the total ionic charge and ε is the permittivity. The Boltzmann equation is expressed as

$$n^{\pm} = n_0 Exp\left[\pm\frac{ez\overline{\Phi}}{K_B T}\right]. \tag{9}$$

Where n_0 represents concentration of ions at the bulk, which is independent of surface electrochemistry, e is the electronic charge, is the charge balance, K_B is the Boltzmann constant, and T is the average temperature of the electrolytic solution.

Introducing the non-dimensional quantities

$$\bar{x} = \frac{x}{\lambda}, \bar{y} = \frac{y}{a}, \bar{u} = \frac{u}{c}, \bar{v} = \frac{v}{c\delta}, \delta = \frac{a}{\lambda}, p = \frac{a^2\bar{p}}{\mu_0 c\lambda},$$
$$\bar{t} = \frac{ct}{\lambda}, \bar{\tau} = \frac{a\tau}{\mu_0 c}, \varphi = \frac{b}{a}, \overline{\Phi} = \frac{\Phi}{a^2},$$
$$R_e = \frac{\rho c a}{\mu}\ and\ \overline{\mu}(\overline{y}) = \frac{\mu(y)}{\mu_0} \tag{10}$$

The equations governing the flow become

$$\frac{\partial u}{\partial x} + \frac{\partial u}{\partial y} = 0. \tag{11}$$

$$R_e\delta\left[u\frac{\partial u}{\partial x} + v\frac{\partial u}{\partial y}\right] = -\frac{\partial p}{\partial x} + \delta\frac{\partial \tau_{xx}}{\partial x} + \frac{\partial \tau_{xy}}{\partial y} - \frac{1}{D_a}(u + 1) + m^2 U_{hs}\Phi. \tag{12}$$

$$\delta^3 R_e\left[u\frac{\partial v}{\partial x} + v\frac{\partial v}{\partial y}\right] = -\frac{\partial p}{\partial x} + \delta^2\frac{\partial \tau_{xy}}{\partial x} + \delta\frac{\partial \tau_{yy}}{\partial y}. \tag{13}$$

where

$$\tau_{xx} = \frac{2\delta\mu(y)}{1+\lambda_1}\left[1+\frac{\delta\lambda_2 c}{a}\left(u\frac{\partial}{\partial x}+v\frac{\partial}{\partial y}\right)\right]\frac{\partial u}{\partial x},$$
$$\tau_{yy} = \frac{2\delta\mu(y)}{(1+\lambda_1)}\left[1+\frac{\delta\lambda_2 c}{a}\left(u\frac{\partial}{\partial x}+v\frac{\partial}{\partial y}\right)\right]\frac{\partial u}{\partial y},$$
$$\tau_{xy} = \frac{\mu(y)}{1+\lambda_1}\left[1+\frac{\delta\lambda_2 c}{a}\left(u\frac{\partial}{\partial x}+v\frac{\partial}{\partial y}\right)\right]\left(\frac{\partial u}{\partial y}+\delta^2\frac{\partial v}{\partial x}\right),$$

Using long wavelength approximation and dropping terms of order δ and higher, Eqs. (11) - (13) reduces to

$$\frac{\partial}{\partial y}\left(\frac{\mu(y)}{1+\lambda_1}\frac{\partial u}{\partial y}\right) - M^2(u+1) + m^2\beta\Phi = \frac{\partial p}{\partial x}. \tag{14}$$

$$\frac{\partial p}{\partial y} = 0 . \tag{15}$$

Where $\mu(y)$ is the viscosity variation on peristaltic flow. For the present analysis, we assume viscosity variation in the form [1]:

$$\mu(y) = e^{-\alpha y} \simeq 1-\alpha y+\alpha^2 y^2, for \alpha \ll 1.$$

The non dimensional boundary conditions are

$$\frac{\partial u}{\partial y} = 0 at y = 0 and u = -1 at y = h. \quad . \tag{16}$$

where $M^2 = \frac{1}{D_a}$, $m = aez\sqrt{\frac{2n_0}{\varepsilon K_B T}}$ is known as the electroosmotic parameter and $\beta = -\frac{E_x\varepsilon\zeta}{\mu_0 c}$ is the maximum electroosmotic velocity. Applying Debye-Hückel linearization approximation, Poisson-Boltzmann equation reduces to

$$\frac{\partial^2\Phi}{\partial y^2} = m^2\Phi. \tag{17}$$

The boundary conditions for electrical potential are

$$\frac{\partial\Phi}{\partial y} = 0 at y = 0, \Phi = 1 at y = h. \tag{18}$$

The solution of the Possion-Boltzmann equation (17) subjected to boundary conditions (18) give rise to

$$\Phi = \frac{Cosh[my]}{Cosh[mh]}. \tag{19}$$

The instantaneous volume flow rate $\overline{Q}(x,t)$ in the laboratory frame between the central line and the wall is

$$\overline{Q}(x,t) = \int_0^h (u+1)dy = q+h. \tag{20}$$

$$Q = \frac{1}{T}\int_0^T \overline{Q}dt = q+1. \tag{21}$$

3. Perturbation solution

Eq. (14) is a nonlinear differential equation so that it is not possible to obtain a closed form solution, we consider the perturbation expansion by writing

$$f = f_0 + \alpha f_1 + \alpha^2 f_2 + \ldots \tag{22}$$

In which f can be replaced by $u and \frac{\partial p}{\partial x}$. And collecting the coefficients of equal power of α.

First we get the zeroth order equation as

$$\frac{1}{1+\lambda_1}\frac{\partial^2 u_0}{\partial y^2} - M^2(u_0+1) + m^2\beta\frac{Cosh(my)}{Cosh(mh)} = \frac{\partial p_0}{\partial x} \tag{23}$$

The corresponding boundary conditions

$$\frac{\partial u_0}{\partial y} = 0, at y = 0$$
$$u_0 = -1 at y = h \tag{24}$$

Second, the first order perturbation equation can be written as

$$\frac{\partial^2 u_1}{\partial y^2} - N^2 u_1 = (1+\lambda_1)\frac{\partial p_1}{\partial x} + \frac{\partial u_0}{\partial y} + y\frac{\partial^2 u_0}{\partial y^2} \tag{25}$$

$$\frac{\partial u_1}{\partial y} = 0, at y = 0$$
$$u_1 = 0 at y = h \tag{26}$$

The second order perturbation equation can be written as

$$\frac{\partial^2 u_2}{\partial y^2} - N^2 u_2 = (1+\lambda_1)\frac{\partial p_2}{\partial x} + \frac{\partial u_1}{\partial y} + y\frac{\partial^2 u_1}{\partial y^2} - 2y\frac{\partial u_0}{\partial y} - y^2\frac{\partial^2 u_0}{\partial y^2} \tag{27}$$

$$\frac{\partial u_2}{\partial y} = 0, aty = 0$$
$$u_2 = 0aty = h \quad (28)$$

From Eqs. (23) and (24) we have

$$u_0 = C_2 Cosh[my] + C_1 Cosh[Ny] - 1 - \frac{dp_0}{dx}\frac{(1+\lambda_1)}{N^2}. \quad (29)$$

Where

$$C_1 = \frac{dp_0}{dx}\frac{(1+\lambda_1)}{N^2 Cosh(Nh)} - \frac{C_2 Cosh(mh)}{Cosh(Nh)}.$$
$$C_2 = \frac{(1+\lambda_1)m^2\beta Sech(mh)}{(m^2-N^2)}.$$

Axial pressure gradient takes the form

$$\frac{dp_0}{dx} = \left(q + \frac{hmN - C_2 NSinh(hm) + C_2 mCosh(hm)Tanh(hN)}{mN}\right)\frac{N^3}{(1+\lambda_1)(-hN+Tanh(hN))}. \quad (30)$$

Similarly we get the first and second order solutions as fallows

$$u_1 = -\frac{1}{4(m-N)^2N^2(m+N)^2}e^{hN}(C_3 + C_4 + C_5C_1)(1 - Tan(hN)). \quad (31)$$

$$C_3 = -4Cosh(Ny)\left((m^2-N^2)^2\frac{dp_1}{dx}(1+\lambda_1) + C_2mN^2\begin{pmatrix} hm(-m^2+N^2)Cosh(hm) + \\ (m^2+N^2)Sinh(hm) - 2mNSinh(hN)\end{pmatrix}\right).$$

$$C_4 = 4Cosh(Nh)\left((m^2-N^2)^2\frac{dp_1}{dx}(1+\lambda_1) + C_2mN^2\begin{pmatrix} m(-m^2+N^2)yCosh(hy) + \\ (m^2+N^2)Sinh(hy) - 2mNSinh(hy)\end{pmatrix}\right).$$

$$C_5 = N(m^2-N^2)^2\begin{pmatrix}(-1+h^2N^2)Cosh(Ny)Sinh(hN) + \\ Cosh(hN)(N(h-y)Cosh(Ny) + (1-N^2y^2)Sinh(Ny))\end{pmatrix}.$$

$$\frac{dp_1}{dx} = -\frac{(4(m-N)^2N^2(m+N)^2)}{C_6}\left(q + \frac{1}{4(m-N)^2N^2(m+N)^2}e^{hN}(C_7 - C_8 - C_9C_1)(1 - Tanh(hN))\right) \quad (32)$$

$$C_6 = \left(e^{hN}\left(4h(m^2-N^2)^2(1+\lambda_1)Cosh(hN) - \frac{4h(m^2-N^2)^2(1+\lambda_1)Cosh(hN)}{N}\right)(1 - Tanh(hN))\right)$$

$$C_7 = -4C_2mN^2Cosh(hN)(-2mCosh(hm) + 2mCosh(hN) + h(m^2-N^2)Sinh(hm))$$

$$C_8 = 4C_2mNSinh(hN)(hm(-m^2+N^2)Cosh(hm) + (m^2+N^2)Sinh(hm) - 2mNSinh(hN))$$

$$C_9 = \frac{1}{2}(m^2-N^2)^2(-1 + 2h^2N^2 + Cosh(2hN) - 2hNSinh(2hN))$$

$$u_2 = -\frac{1}{96(m-N)^4N^3(m+N)^4}e^{hN}\begin{pmatrix}24\begin{pmatrix}2C_2mN^4Cosh(hN)C_{10} + (m-N)^2 \\ (m+N)^2C_{11}C_{12}(1 - Tanh(hN))\end{pmatrix} \\ +(m-N)^4N(m+N)^4C_{13}\end{pmatrix}(1 - Tanh(hN)). \quad (33)$$

$$C_{10} = \begin{pmatrix}-2mN(4m^2 + 8N^2 + (m^2-N^2)^2y^2)Cosh(my) + mN(8m^2 + 16N^2 - (m^2-N^2)^2y^2)Cosh(Ny) \\ -4N(-2m^4 + m^2N^2 + N^4)ySinh(my) - m(m^2-N^2)^2ySinh(Ny)\end{pmatrix}.$$

$$C_{11} = \begin{pmatrix}-(m^2-N^2)^2\frac{dp_1}{dx}(1+\lambda_1) + C_2mN^2 \\ (hm(m-N)(m+N)Cosh(hm) - (m^2+N^2)Sinh(hm) + 2mNSinh(hN))\end{pmatrix}.$$

$$C_{12} = (NyCosh(Ny) + (-1 + y^2N^2)Sinh(Ny)).$$

$$C_{13} = \begin{pmatrix}\begin{pmatrix}6(-1+h^2N^2)Sinh(hN)(NyCosh(Ny) + (-1+h^2N^2)Sinh(yN)) + \\ NCosh(hN)\begin{pmatrix}3Ny(2h + 5y - N^2y^3)Cosh(Ny) + \\ (-6h - 15y + 6hN^2y^2 - 2N^2y^3)Sinh(Ny)\end{pmatrix}\end{pmatrix} \\ C_1 - 96(1+\lambda_1)Cosh(hN)(-1 + Cosh(Ny))\frac{dp_2}{dx}\end{pmatrix}.$$

$$\frac{dp_2}{dx} = \frac{N^3}{C_{17}}\left(q + \frac{1}{96(m-N)^4N^3(m+N)^4}e^{hN}(24(C_{14} + C_{15}) + C_{16}C_1)(1 - Tanh(hN)\right). \quad (34)$$

$$C_{14} = -2C_2 mN^2 Cosh(hN)\begin{pmatrix} -12hmN^3(m^2-N^2)Cosh(hm) - hmN(m^2-N^2)^2 Cosh(hN) \\ +20m^2N^3 Sinh(hm) + 2h^2m^4N^3 Sinh(hm) + 4N^5 Sinh(hm) - \\ 4h^2m^2N^5 Sinh(hm) + 2h^2N^7 Sinh(hm) + m^5 Sinh(hN) \\ -10m^3N^2 Sinh(hN) + h^2m^5N^2 Sinh(hN) - 15mN^4 Sinh(hN) \\ -2h^2m^3N^4 Sinh(hN) + h^2mN^6 Sinh(hN) \end{pmatrix}.$$

$$C_{15} = h(m-N)^2(m+N)^2(hNCosh(hN) - Sinh(hN))\begin{pmatrix} -(m^2-N^2)^2\frac{dp_1}{dx}(1+\lambda_1) + C_2 mN^2 \\ \begin{pmatrix} hm(m-N)(m+N)Cosh(hm) - \\ (m^2+N^2)Sinh(hm) + 2mNSinh(hN) \end{pmatrix} \end{pmatrix}.$$

$$C_{16} = \frac{1}{2}(m-N)^4(m+N)^4\begin{pmatrix} hN(9+22h^2N^2) + hN(21+10h^2N^2)Cosh(2hN) \\ +3(-5-9h^2N^2+h^4N^4)Sinh(2hN) \end{pmatrix}.$$

$$C_{17} = e^{hN}(1+\lambda_1)Cosh(hN)(-hN + Sinh(hN))(1 - Tanh(hN)).$$

Thus, we can get

$$u = u_0 + \alpha u_1 + \alpha^2 u_2.$$

$$\frac{dp}{dx} = \frac{dp_0}{dx} + \alpha\frac{dp_1}{dx} + \alpha^2\frac{dp_2}{dx}.$$

The pressure rise per wave length is given by

$$\Delta p = \int_0^1 \left(\frac{dp}{dx}\right) dx.$$

The volume flux q through each cross section of the channel in the wave frame is given by

$$q = \int_0^h u dy$$

4. Results and discussion

In order to estimate the present analysis, equations are solved by perturbation method. To study the effects of Jeffrey fluid parameterλ_1, Electro-osmotic parameter m, Electroosmotic velocity and Viscosity parameter α on pressure rise and friction force per wave length are solved numerically, Numerical simulation are performed by using MATHEMATICA software. We have presented a set of Figures, which describe the effects of various parameters of interest on flow quantities such as pressure gradient and pressure rise per wavelength.

Figures 1(a)-(d)show the variations of the axial pressure gradient $\frac{dp}{dx}$ along the length of the channel, which has oscillatory behavior in the whole range of the x -axis for all other parameters. From Figure 1(a) it is seen that for fixed values of all other parameters, the axial pressure gradient decreases with increase in Jeffrey fluid parameter. The effect of electro-osmotic parameter is depicted in Figure 1 (b). It is noted that axial pressure gradient enhances with increasing Electro-osmotic parameter. From Figure 1(c) it is observed that, with an increase in the Electroosmotic velocity the axial pressure gradient increases. The effect of Viscosity parameter is depicted in Figure 1 (d). It is noted that axial pressure gradient decreases with increasing Viscosity.

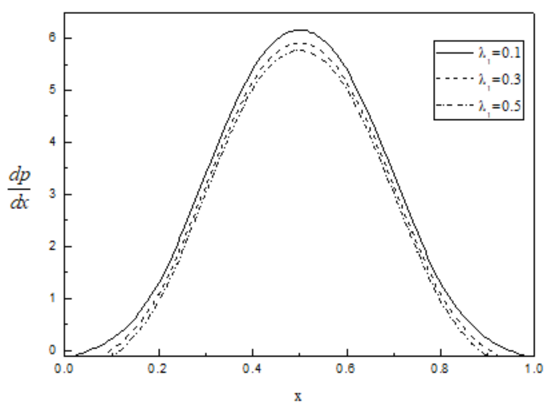

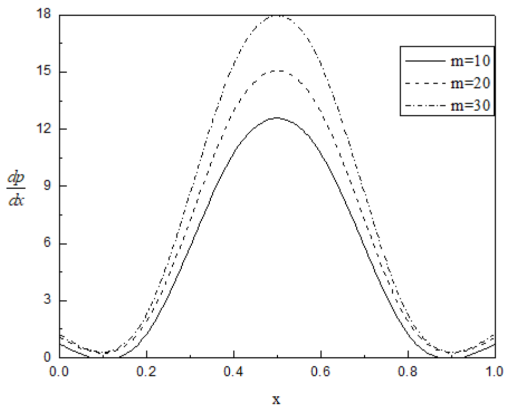

(a) (b)

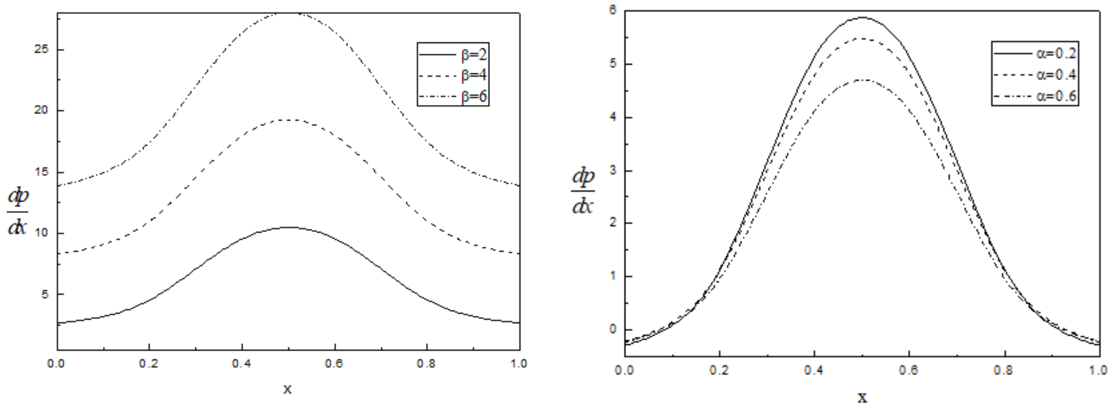

(c) (d)

Fig. 1. Axial pressure gradient for (a) $\varphi = 0.2, m = 2, \alpha = 0.1 and \beta = 1$. (b) $\varphi = 0.6, \lambda = 0.1, \alpha = 0.1 and \beta = 1$. (c)$\varphi = 0.2, \lambda = 1, \alpha = 0.2 and m = 2$. (d)$\varphi = 0.2, \lambda = 0.3, \beta = 1 and m = 2$.

Figures 2(a)-(d) give the variations pressure rise with time-averaged flux. It can be noticed from Figure 2(a) that for an increase in Jeffrey fluid parameter causes the diminish in pressure rise. The effect of electro-osmotic parameter on pumping characteristics is depicted in Figure 2 (b). It is noted that Electro-osmotic parameter significantly enhance pressure differences with increasing averaged volumetric flow rate in the pumping region $\Delta p > 0$, the free pumping region $\Delta p = 0$ and the augmented pumping region $\Delta p < 0$.The effect of Electro-osmotic velocity is depicted in Figure 2 (c). It is noted that pressure rise elevates with increasing Electro-osmotic velocity in the pumping region, the free pumping region and the augmented pumping region. From Figure 2(d) it is revealed that with an increase in the Viscosity there is decrease in the pumping region, the free pumping region and enhances in the augmented pumping region.

Conclusion

We have investigated the impact of electro kinetic variable viscosity on peristaltic transfer of Jeffrey fluid. Closed form solutions are derived for the pressure gradient and pressure rise. The main observations of the present work are as follows.

It is observed that pressure gradient decreases with the increase of Jeffrey fluid parameter λ_1 and viscosity parameter α. while it increases by increasing m and β .

It is observed that pressure rise decreases with the increase in Jeffrey fluid parameter λ_1 and viscosity parameter. However it increases with an increase in electro-osmotic parameter m and electro-osmotic velocity β.

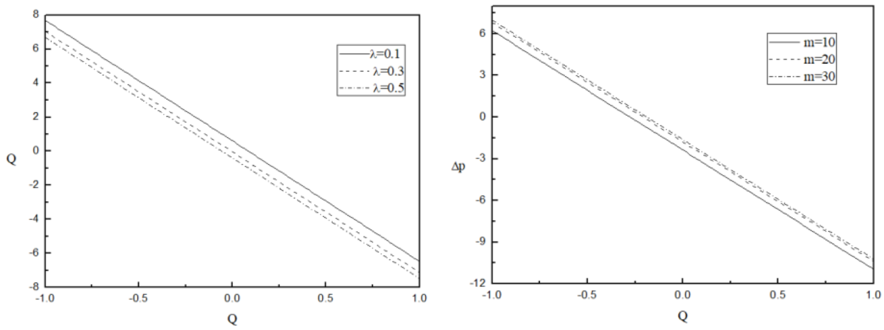

(a) (b)

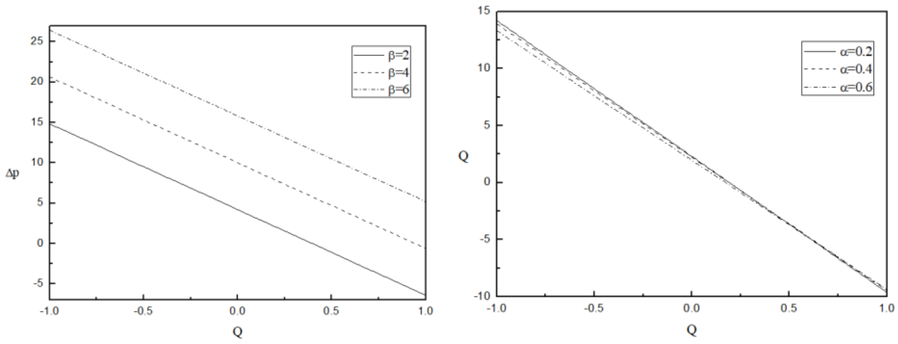

(c) (d)

Fig. 2. Pressure rise with time-averaged flux for (a) $\varphi = 0.6, m = 2.5, \alpha = 0.1 and \beta = 1.$ (b) $\varphi = 0.2, \lambda = 0.1, \alpha = 0.1 and \beta = 1.$ (c)$\varphi = 0.2, \lambda = 0.1, \alpha = 0.2 and m = 2.$ (d)$\varphi = 0.1, \lambda = 0.1, \beta = 1 and m = 2.$

REFERENCES

1. T.W. Latham : Fluid motion in a peristaltic pump. M. Sc. Thesis. MIT. Cambridge. M. A (1966).
2. K. K. Raju., R. Devanathan : Peristaltic motion of a non-Newtonian fluid: Part I. Rheol. Acta. 11(1972), 170–178.
3. Laxmi Devindrappa., N. B. Naduvinamani : Peristaltic transport of a Bingham fluid with permeable walls by Adomian decomposition method. Journal of applied science and computations. 5(2018), 908-918.
4. Laxmi Devindrappa., N. B. Naduvinamani : Hall current effects on Peristaltic transport of a conducting Bingham fluid with permeable walls by Adomian decomposition method. International Journal of Scientific research and reviews. Volume 7(2018), 179 -197.
5. S.K. Asha., G. Sunitha : Effects of joule heating and MHD on peristaltic blood flow of Eyring-Powell nonofluid in a non-uniform channel. Journal of Taibah University for science. 13(2019), 155-168.
6. S. K. Asha., C.K. Deepa : Peristaltic flow of a third grade fluid accounting joule heating and magnetic field. World scientific news. 137(2019), 1-17.
7. V.P.Rathod., M. Mahadev : Interaction of heat transfer and peristaltic pumping of fractional second grade fluid through a vertical cylindrical tube. Thermal science. 18(2014), 1109-1118.
8. V.P. Rathod., D. Laxmi : Effects of heat transfer on the peristaltic MHD flow of a Bingham fluid through a porous medium in a channel. International journal of Biomathematics. 7(2014), 1450060.
9. B.B. Divya., G. Manjunatha., C. Rajashekhar., Hanumesh vaidya., K.V Prasad : Hemodynamics of variable liquid properties on the MHD peristaltic mechanism of Jeffery fluid with heat and mass transfer. Alexandria Engineering Journal. 59(2020), 693-706.
10. F. M. Abbasi., T. Hayat., S.A. Shehzad., F. Alsaadi., N. Altoaibi : Hydromagnetic peristaltic transport of copper-water nanofluid with temperature-dependent effective viscosity. Particuology. (2016).
11. N.S. Akbar., S. Nadeem : Simulation of variable viscosity and Jeffrey fluid model for blood flow through a tapered artery with a stenosis. Commun. Theor. Phys. 57(2012), 133–140.
12. S. Farooq., M. Awais., Moniza Naseem., T. Hayat., B. Ahmad : Magnetohydrodynamic peristalsis of variable viscosity Jeffrey fluid with heat and mass transfer. Nuclear Engineering and Technology. (2017).
13. S. Nadeem., N. S. Akbar : Peristaltic flow of a Jeffrey fluid with Variable Viscosity in an asymmetric channel. Z. Naturforsch. 64(2009), 713-722.
14. R. E. Abo-Elkhair., KH.S. Mekheimer., A. M. A. Maowad : Combine impacts of electrokinetic variable viscosity and partial slip on peristaltic MHD flow through a micro-channel. Iranian Journal of Science and Technology A Science. 43(2019), 201-212.
15. Laxmi Devindrappa., N. B. Naduvinamani., G.C. Shit : peristaltically induced Electroosmotic flow of Jeffrey fluid with Zeta potential and Navier- Slip at the wall. International journal of Innovative Technology and Exploring Engineering. 8(2019), 1324-1329.
16. Laxmi Devindrappa., N. B. Naduvinamani : Electrokinetic flow of peristaltic transport of Jeffrey fluid in a porous channel. Journal of Information and Computational Science. 9 (2019).
17. A. Sharma., D. Tripathi., R. K. Sharma., A.K. Tiwari : Analysis of double diffusive convection in electroosmosis regulated peristaltic transport of nanofluids. Physica A. 535(2019), 122-148.
18. N.K. Ranjit., G. C. Shit., D. Tripathi : Entropy generation and Joule heating of two layered electroosmotic flow in

the peristaltically induced micro-channel. International Journal of Mechanical Sciences. 153–154 (2019), 430–444.

19. A. Mondal., G. C. Shit : Electro-osmotic flow and heat transfer in a slowly varying asymmetric micro-channel with Joule heating effects. Fluid Dynamics Research. 50(2018), 065502.
20. N. Ranjit., G. C. Shit : Entropy generation on electromagnet hydrodynamic flow through a porous asymmetric micro-channel. European Journal of Mechanics / B Fluids. 77(2019), 135–147.